

## EXPERIMENTAL AND MICROMECHANICAL APPROACH TO ELASTIC PROPERTIES OF ARTIFICIALLY CEMENTED SAND

**Samir Maghous, Anderson Fonini, Nilo C. Consoli and Vanessa F. Pasa Dutra**

*Centro de Mecânica Aplicada e Computacional, Universidade Federal do Rio Grande do Sul, Oswaldo Aranha 99, Porto Alegre, Brasil, samir.maghous@ufrgs.br, <http://www.ufrgs.br/cemacom/>*

**Keywords:** Artificially cemented sand, elastic properties, experiments, micromechanics.

**Abstract.** Cement treatment of granular soils is a widely used technique in the field of soil improvement, which proved effective for ground stabilization in a large variety of geotechnical works. The present study investigates some aspects of the mechanical behavior of artificially cemented sands (ACS) by means of experimental characterization and micromechanics-based modeling. Particular emphasis is given to the increase in elastic stiffness brought by cementation. Based on the concept of a fictitious continuum medium and the homogenization theory, the effective elastic properties of ACS are evaluated using the Mori-Tanaka and self-consistent schemes. The estimates derived from the direct implementation of both schemes underestimate the increase in stiffening induced by cementation. Corrective terms have been therefore introduced and successively calibrated from the experimental data obtained by means of bender element tests performed on specimens of sand reinforced by different amounts of cement. It has been notably found from the comparison with experimental results that the empirically corrected Mori-Tanaka scheme is better indicated for capturing the stiffness improvement brought by cement addition.

## 1 INTRODUCTION

Cement treatment of granular soils is a widely used technique in the field of soil improvement, which proved effective for ground stabilization in a large variety of geotechnical works. This kind of reinforcement have been notably applied in pavement base layers, pipe bedding, slope protection for earth dam, as a base layer to shallow foundations and to prevent sand liquefaction.

Soil-cement is a geo-composite elaborated from highly compacted mixture of granular soil, Portland cement and water. As the cement hydrates, the stiffness and strength of the mixture increase while its permeability reduces, leading to a net improving of the engineering properties of the raw soil. One of the main advantages in improving locally fine-grained soils with cement is to avoid the need of bringing from away great volumes of sand and gravelly materials, which might involve high costs that are hardly compatible with the economical constraints.

During the last decades, important laboratory studies have significantly contributed to better understanding the physical mechanisms and macroscopic parameters affecting the behavior of artificially cemented sand, referred to as ACS throughout the paper.

Recent research studies on granular soil-cement blends have sought to establish experimentally a dosage methodology based on the definition of some key parameters that control the mechanical properties of ACS at macroscopic level. It has been notably found that the porosity/cement ratio plays a fundamental role in the assessment of the target stiffness and strength (Consoli et al., 2012). Representative contributions on this subject are due to works by Consoli and co-authors (see for instance references Consoli et al., 2007; 2010; 2012).

In spite of the common use of Portland cement in the improvement of local soils and a large amount of experimental works dedicated to characterize many aspects of ACS behavior, there is still a lack of theoretical-based models that could help to accurately analyze the mechanical response of geo-structures involving ACS materials.

In the context of micromechanical modeling, there are few approaches that have dealt with the formulation of the behavior of cement-sand composites. These works specifically focused on the situation of sand reinforced by cement grouting (Maalej, 2007; Bouchelaghem et al., 2010) and not on artificially cement sand that is the purpose of this paper. It should be emphasized that the distinction between the artificially cemented sand and grouted sand is mainly related to type and degree of cementation, which is usually significantly lower for artificially cement sand. In addition, the volume fraction of cement is controlled in ACS, while it varies in space along the grouted domain due to particle filtration. (e.g., Maghous et al., 2007).

The present paper investigates some aspects of the mechanical behavior of ACS by means of an experimental and theoretical analysis. More precisely, the objective herein is twofold. First, to formulate, within a micromechanical and experimental settings, the elastic properties of ACS at macroscopic level. Second, to discuss the relevance of the micromechanical modeling basis, particularly the morphological description of ACS at micro-scale, in light of the comparison between experimental and model results.

## 2 EXPERIMENTAL PROGRAM

The experimental program was carried out in two parts. First, the geotechnical properties of the studied soil were characterized. Then a number of Bender element tests were carried out and the elastic properties of the ACS was determined.

## 2.1 Materials

The Osorio sand used in the testing was obtained from the region of Porto Alegre, in Southern Brazil, and is classified (ASTM D2487, 1993) as a non-plastic uniform fine sand (SP) with rounded particle shape and specific gravity of the solids equal to 2.65. Mineralogical analysis showed that sand particles are predominantly quartz. The grain size is purely fine sand with a mean effective diameter ( $D_{50}$ ) of 0.16 mm, and with uniformity and curvature coefficients of 2.1 and 1.0, respectively. The minimum and maximum void ratios are 0.6 and 0.9, respectively. The angle of shearing resistance at constant volume is about  $30^\circ$ .

High early strength Portland cement (Type III according to ASTM C150, 2009) was used as the cementing agent. Its fast gain of strength allowed the adoption of 7 days as the curing time. The corresponding unconfined compressive strength at 7 days curing is equivalent to the unconfined compressive strength at 28 days curing of an ordinary Portland cement (Type I). The specific gravity of cement grains is 3.15. Distilled water was used for the characterization tests and tap water for molding specimens.

## 2.2 Methods

Molding and curing of specimen as well as testing procedures are summarized below.

### 2.2.1 Molding and curing of specimens

For all the ACS tests, cylindrical specimens 70 mm in diameter and 140 mm high were used. A target dry unit weight for a given specimen was then established through the dry mass of soil-cement divided by the total volume of the specimen. In order to keep the dry unit weight of the specimens constant with increasing cement content, a small portion of the soil was replaced by cement. Calculation of the porosity is therefore based on the specific gravity of the composite, which is computed from the soil and cement percentages in the specimens.

After the soil, cement and water were weighed, the soil and cement were mixed until the mixture acquired a uniform consistency. The water was then added while continuing the mixture process until a homogeneous paste was created. The amount of cement for each mixture was calculated based on the mass of dry soil and the moisture content. Cement content is defined as the mass of cement divided by the mass of dry soil. The moisture content is defined as the mass of water divided by the mass of solids (sand particles and cement powder).

The specimen was then statically compacted in three layers inside a cylindrical stainless steel mould, which was lubricated, so that each layer reached the target density. The top of each layer was slightly scarified. After the molding process, the specimen was immediately extracted from the mould and its weight, diameter and height were measured. The samples were then placed inside plastic bags to avoid significant variations of moisture content. They were cured for 7 days in a humid room at  $23^\circ\text{C} \pm 2^\circ\text{C}$  and relative humidity above 95%.

### 2.2.2 Bender element tests

Bender elements tests are currently a standard technique for measurement of the stiffness of a soil at very small strains. Piezoceramic transmitter and receiver were installed on the top and bottom of each ACS specimen. They consisted in T-shaped pairs of bender/extender elements (BE) used for emission and reception of shear “S” waves (2 to 20 kHz) and compression “P” waves (20 to 80 kHz). The bender/extender elements penetrated the specimen by 3 mm at each end. The procedure allows for direct measurement of elastic shear and oedometric

moduli of ACS.

The principle of BE testing is simple (Viggiani and Atkinson, 1995), but a clear identification of travel time is not always possible. Clayton (2011) summarizes the wide range of issues that have been identified in the manufacture and use of bender elements. For the considered sand-cement mixtures, a time domain method of identification for first arrivals was adopted.

Single sine-wave input pulses were used at pre-set frequencies of 2, 4, 6, 8, 20, 40, 60 and 80 kHz, which covered the range of resonant frequencies of the sample-BE system. The output signals were captured on an oscilloscope, transferred directly to the PC and plotted to a common time base using Wavestar software. The first arrival of the wave was taken (on the basis of previous calibration) as the point at which the wave descended, with low-noise, higher-frequency results being preferred in order to avoid near-field effects.

### 2.2.3 Tests Program

The program was defined with the objective to evaluate separately the influence of the cement content and porosity on the initial stiffness of artificially cemented soils. The molding points for testing the initial stiffness parameters of the Osorio sand were chosen considering four values of relative density, ranging from low relative density sand (DR=10%), to high relative density sand (DR=90%) with the same moisture contents (10%). They correspond to void ratios respectively equal to  $e=0.87$ ,  $e=0.80$ ,  $e=0.70$  and  $e=0.63$ . Each point was molded with five different cement contents: 1%, 2%, 3%, 5% and 7%. These percentages were chosen considering the Brazilian and international experience with soil-cement (e.g., Mitchell, 1981; Consoli et al., 2006; 2007).

## 3 FUNDAMENTALS OF CONTINUUM MICROMECHANICS

This section provides a very brief introduction to micromechanics and homogenization in linear elasticity. The interested reader may refer for instance to Dormieux et al. (2006a) for a more detailed presentation. The last part of the section deals with the application of continuum micromechanics to describe elastic properties of Osorio sand.

### 3.1 Basic concepts

The homogenization theory aims at estimating the effective behavior of composite materials. The main interest of the approach lies on the possibility to use the obtained effective behavior to perform computations at the scale of the homogeneous structure by reasoning on the so-defined homogenized structure instead over the original heterogeneous one (Figure 1). In continuum micromechanics, the material is understood as a macro-homogeneous but heterogeneous body at the scale adopted for material description. A central concept of the homogenization procedure is the existence of a representative elementary volume (REV) of characteristic size  $l$  which must comply with two conditions:

- to be elementary, which means that it is small enough compared to the size  $L$  of the structure;
- to be representative, that is to be large enough compared to the size  $d$  characterizing the heterogeneity of the microstructure.

The above conditions represent the so-called condition for scale separation  $d \ll l \ll L$ , necessary for the concept of REV to be valid (Zaoui, 2002).

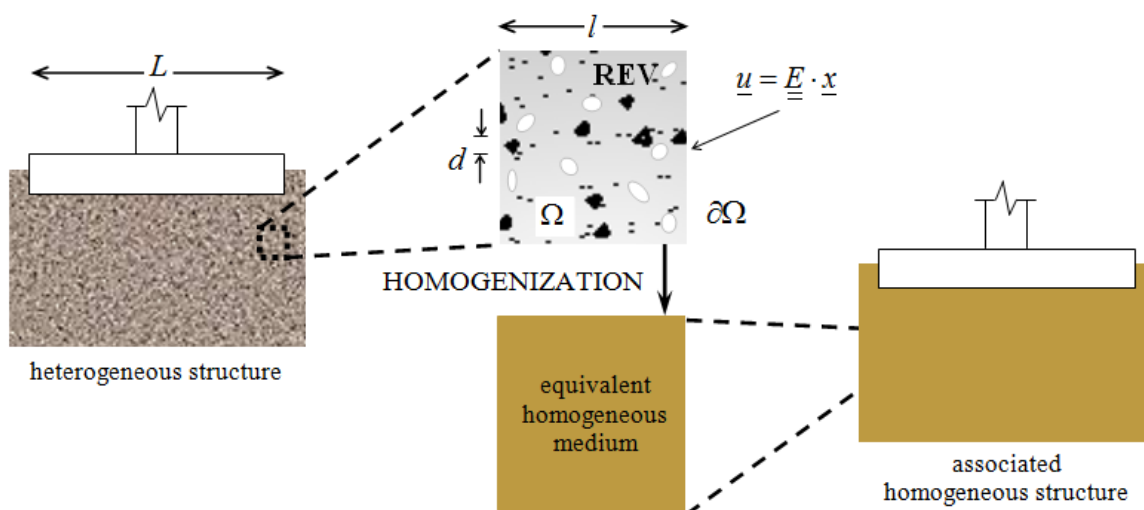


Figure 1: Schematic description of the homogenization process.

In general, the microstructure within each REV is so complicated that it cannot be described in detail. Therefore, quasi-homogeneous sub-domains with known physical quantities (such as volume fraction, elastic or strength properties) are reasonably defined within the REV. They are referred to as material phases. The central objective of continuum micromechanics is to estimate the mechanical properties of the material defined on the REV from the aforementioned phase properties.

The loading of the REV is defined by means of uniform strain boundary conditions (Figure 1).

$$\underline{u}(x) = \underline{\underline{E}} \cdot \underline{x} \quad \text{on } \partial\Omega \tag{1}$$

where  $\underline{\underline{E}}$  denotes the macroscopic strain tensor and  $\underline{x}$  is the position vector labeling points within the REV  $\Omega$  or located along its boundary  $\partial\Omega$ . In the framework of homogenization of random composite media applied to linear elasticity, each phase ( $r$ ) is characterized by its four-order stiffness tensor  $\underline{\underline{c}}^r$  relating the stress tensor to strain tensor.

The formulation of the macroscopic elastic behavior stems from the resolution of the following concentration problem (Suquet, 1987):

$$\begin{cases} \text{div } \underline{\underline{\sigma}} = 0 & \text{on } \Omega \\ \underline{\underline{\sigma}} = \underline{\underline{c}}(\underline{x}) : \underline{\underline{\varepsilon}} & \text{on } \Omega \\ \underline{u} = \underline{\underline{E}} \cdot \underline{x} & \text{on } \partial\Omega \end{cases} \tag{2}$$

From linearity arguments, it appears that the local strain  $\underline{\underline{\varepsilon}}(\underline{x})$  is proportional to the macroscopic strain  $\underline{\underline{E}}$  through strain concentration tensor  $\underline{\underline{A}}(\underline{x})$ , i.e.  $\underline{\underline{\varepsilon}}(\underline{x}) = \underline{\underline{A}}(\underline{x}) : \underline{\underline{E}}$ . Averaging the local elastic constitutive equation over the REV yields the expression of the homogenized stiffness tensor:

$$\underline{\underline{C}}^{\text{hom}} = \langle \underline{\underline{c}} : \underline{\underline{A}} \rangle = \sum_r f^r \underline{\underline{c}}^r : \langle \underline{\underline{A}} \rangle_r \tag{3}$$

In the above relationship,  $f^r$  stands for the volume fraction of phase ( $r$ ),  $\underline{\underline{c}}^r$  is the

stiffness tensor of phase ( $r$ ) and  $\langle a \rangle$  (resp.  $\langle a \rangle_r$ ) refers to the volume average of field  $a$  over the REV (resp. over the domain occupied by phase ( $r$ )). Interestingly noting, a kinematically compatible strain field complies with the average rule  $\langle \underline{\underline{\varepsilon}} \rangle = \underline{\underline{E}}$ .

As emphasized by Eq. 3, the determination of the overall elasticity tensor requires being able to compute estimates of the average of strain concentration tensor over each phase ( $r$ ). The latter estimates are in practice obtained by resorting to an appropriate homogenization scheme integrating some information on the morphology. In the Eshelby-based approach (Eshelby, 1957), the average strain concentration tensor  $\langle \underline{\underline{A}} \rangle_r$  is estimated from the uniform strain that establishes in an ellipsoidal inclusion embedded into an infinite medium (reference medium) with stiffness  $\underline{\underline{\zeta}}^0$  subjected to uniform strain boundary conditions at infinity of the form  $\underline{\underline{u}}(\underline{\underline{x}}) = \underline{\underline{E}}^\infty \cdot \underline{\underline{x}}$  for  $|\underline{\underline{x}}| \rightarrow +\infty$ . This reference strain  $\underline{\underline{E}}^\infty$  is related to the macroscopic strain  $\underline{\underline{E}}$  applied at the boundary of the REV according to the average strain rule  $\langle \underline{\underline{\varepsilon}} \rangle = \underline{\underline{E}}$ . The shape of the ellipsoid representing a given phase and the stiffness  $\underline{\underline{\zeta}}^0$  both depend on the morphology of the microstructure. In the framework of Eshelby-based approach, the estimate of  $\langle \underline{\underline{A}} \rangle_r$  reads

$$\langle \underline{\underline{A}} \rangle_r^{\text{est}} = \left[ \underline{\underline{1}} + \underline{\underline{P}}^{0,r} : (\underline{\underline{\zeta}}^r - \underline{\underline{\zeta}}^0) \right]^{-1} : \left\langle \left[ \underline{\underline{1}} + \underline{\underline{P}}^0 : (\underline{\underline{\zeta}} - \underline{\underline{\zeta}}^0) \right]^{-1} \right\rangle^{-1} \quad (4)$$

where  $\underline{\underline{P}}^{0,r}$  is the fourth-order Hill tensor. It depends on the stiffness  $\underline{\underline{\zeta}}^0$  of the reference matrix as well as on the shape and orientation of the considered inclusion. Closed-form analytical expressions of Hill tensor  $\underline{\underline{P}}^{0,r}$ , or equivalently of the so-called Eshelby tensor  $\underline{\underline{S}}^{0,r} = \underline{\underline{P}}^{0,r} : \underline{\underline{\zeta}}^0$ , are available for particular configurations of material symmetry and inclusion shape (see for instance Mura, 1987).

Substitution of Eq. 4 into Eq. 3 yields the sought estimate for the homogenized (macroscopic) elasticity tensor:

$$\underline{\underline{C}}^{\text{est}} = \left\langle \underline{\underline{\zeta}} : \left[ \underline{\underline{1}} + \underline{\underline{P}} : (\underline{\underline{\zeta}} - \underline{\underline{\zeta}}^0) \right]^{-1} : \left\langle \left[ \underline{\underline{1}} + \underline{\underline{P}}^0 : (\underline{\underline{\zeta}} - \underline{\underline{\zeta}}^0) \right]^{-1} \right\rangle^{-1} \right\rangle \quad (5)$$

When a particular continuous phase ( $m$ ) surrounding all the other phases can be clearly identified, the Mori-Tanaka scheme (Mori and Tanaka, 1973; Benveniste, 1987) considers it as the reference medium:  $\underline{\underline{\zeta}}^0 = \underline{\underline{\zeta}}^m$ . On the other hand, the self-consistent scheme (Hill, 1965; Budiansky, 1965) adopts the searched homogenized material as the reference medium:  $\underline{\underline{\zeta}}^0 = \underline{\underline{C}}^{\text{hom}}$ . The self-consistent scheme is classically used to model perfectly disordered materials such as polycrystal-like microstructures.

### 3.2 Micromechanical modeling of Osorio sand elastic properties

This section deals with the application of continuum micromechanics tools to estimate the elastic properties of Osorio sand.

To estimate the effective elastic moduli of artificially cemented sand (ACS) through homogenization of random media, we need first to develop a framework in which concepts of continuum micromechanics can apply. Since sand is a granular material, the latter is modeled following the idea presented in Maalej (2007) who introduced the concept of elastic fictitious

continuous porous medium to represent sand material.

At the scale of REV, the solid phase of sand consists in a set of discrete grains in mutual contact (Figure 2) and the global behavior is mainly controlled by the intergranular interface contacts. A continuous description of sand at the microscopic level is achieved introducing an equivalent fictitious continuous porous medium (Figure 2b) fulfilling the following conditions:

- it has the same value of pore volume fraction ( porosity)  $\eta_0$  than the considered sand;
- its effective elastic properties are equivalent to those of the considered sand.

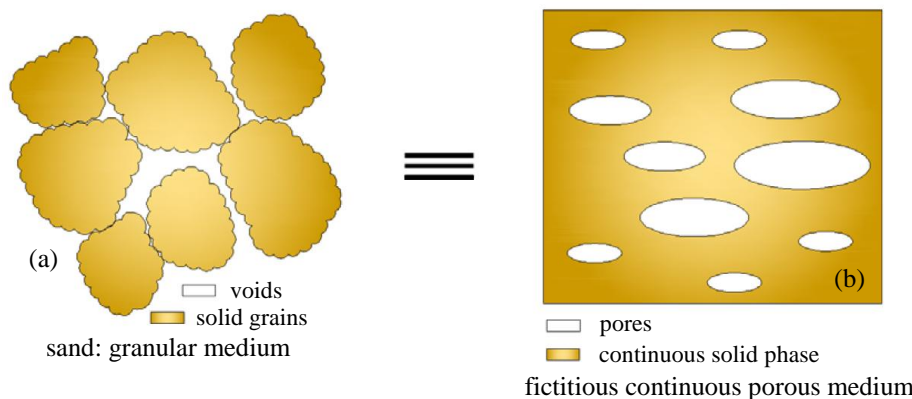


Figure 2: Description of sand material by means of an equivalent fictitious continuous porous medium.

This fictitious porous medium is described by a homogeneous continuous solid phase with isotropic elastic properties,  $k^s$  denoting the bulk modulus and  $\mu^s$  the shear modulus. In the homogenization schemes that will be used in the subsequent analysis, the pore space the solid phase is represented by spherical inclusions. The homogenized medium is therefore isotropic and the homogenization process reduces to the determination of bulk and shear moduli  $k^{est}$  and  $\mu^{est}$  of the fictitious continuum material. Starting from the elastic properties of Osorio sand that are known from experimental measurements, the homogenization procedure will actually be used to evaluate the elastic properties  $k^s$  and  $\mu^s$  of the fictitious continuous solid phase. Two homogenization schemes are employed: the Mori-Tanaka scheme and the self-consistent scheme.

In the Mori-Tanaka scheme, the reference medium is coincident with the solid phase. Eq. 5 used with  $\zeta^0 = \zeta^s(k^s, \mu^s)$  yields the following estimates for fictitious material

$$k^{MT} = \frac{4(1-\eta_0)}{3\eta_0 + 4\frac{\mu^s}{k^s}} \mu^s \quad \mu^{MT} = \frac{(1-\eta_0)\left(9 + 8\frac{\mu^s}{k^s}\right)}{9\left(1 + \frac{2}{3}\eta_0\right) + 8\frac{\mu^s}{k^s}\left(1 + \frac{3}{2}\eta_0\right)} \mu^s \quad (6)$$

Expressing the elastic equivalency between Osorio sand and associated fictitious continuous medium, that is  $k^{sand} = k^{MT}$  and  $\mu^{sand} = \mu^{MT}$ , and assuming that the sand properties are known, allow for the calculation of  $(k^s, \mu^s)$  associated with the Mori-Tanaka estimate

$$k^s = \frac{k^{sand} \left( \mu^{sand} (12\eta_0 + 8) + k^{sand} (6\eta_0 - 9) + \mathcal{Q} \right)}{(1-\eta_0) \left( \mu^{sand} (12\eta_0 + 8) - k^{sand} (6\eta_0 + 9) + \mathcal{Q} \right)} \quad \mu^s = \frac{\mu^{sand} (12\eta_0 + 8) + k^{sand} (6\eta_0 - 9) + \mathcal{Q}}{16(1-\eta_0)} \quad (7)$$

where

$$\mathcal{Q} = \sqrt{(12\mu^{sand} - 6k^{sand})^2 \eta_0^2 + 12\eta_0 (16\mu^{sand^2} - 10\mu^{sand} k^{sand} - 9k^{sand^2}) + (8\mu^{sand} + 9k^{sand})^2} \quad (8)$$

In the self-consistent model, the homogenized medium is considered as the reference medium. Eq. 5 used with  $\zeta^0 = \zeta^{hom}$  yields the following estimates for fictitious material (Dormieux et al., 2006b):

$$k^{SC} = (1 - \eta_0) \frac{k^s}{1 + \alpha \frac{k^s - k^{SC}}{k^{SC}}} \quad \mu^{SC} = (1 - \eta_0) \frac{\mu^s}{1 + \beta \frac{\mu^s - \mu^{SC}}{\mu^{SC}}} \quad (9)$$

with

$$\alpha = \frac{3k^{SC}}{3k^{SC} + 4\mu^{SC}} \quad \text{and} \quad \beta = \frac{6(k^{SC} + 2\mu^{SC})}{5(3k^{SC} + 4\mu^{SC})} \quad (10)$$

Similarly to the situation of Mori-Tanaka estimate, we proceed to the evaluation of elastic properties of solid phase from the knowledge of those of Osorio sand. It is readily obtained that

$$k^s = \frac{4k^{sand} \mu^{sand}}{4\mu^{sand} (1 - \eta_0) - 3k^{sand} \eta_0} \quad \mu^s = \frac{(9k^{sand} + 8\mu^{sand}) \mu^{sand}}{3k^{sand} (3 - 5\eta_0) + 4\mu^{sand} (2 - 5\eta_0)} \quad (11)$$

Eq. 7 and Eq. 11 theoretically allow evaluating the elastic properties of the fictitious solid phase.

From a practical viewpoint, only the shear modulus  $\mu^{sand}$  is available from laboratory tests in the case of Osorio sand. This is principally due to the difficulty to deal experimentally with unconfined specimen of sand. Following the idea explored by Maalej (2007), which has adopted the approximation that Poisson ratio  $\nu^s$  of the fictitious solid phase remains constant during a loading cycle. This assumption is based on experimental and modeling results presented by Emeriault and Cambon (1996). For simplicity, we therefore adopt a value close to  $\nu^s = 0.3$ . Accordingly,  $k^s$  and  $\mu^s$  can be related by means a constant coefficient

$$k^s / \mu^s = \lambda \quad \text{with} \quad \lambda = 2(1 + \nu^s) / 3(1 - 2\nu^s) \quad (12)$$

This coefficient reads  $\lambda \approx 13/6$  if a typical value close to 0.3 is for instance adopted for  $\nu^s$ . The values of shear modulus experimentally measured for Osorio sand are given in Table 1.

Void ratio $e$	Porosity $\eta_0$	Shear modulus $\mu^{sand}$ (MPa)
0.63	0.39	25.0
0.70	0.41	22.7
0.80	0.44	20.5
0.87	0.47	18.3

Table 1: Shear modulus of tested Osorio sand.

The estimates of the elastic properties of the fictitious solid that are predicted by the use of

Mori-Tanaka and self-consistent schemes are plotted in Figure 3a and Figure 3b. These figures display the variations of the bulk  $k^s$  and the shear  $\mu^s$  moduli versus the Osorio sand porosity  $\eta_0$ .

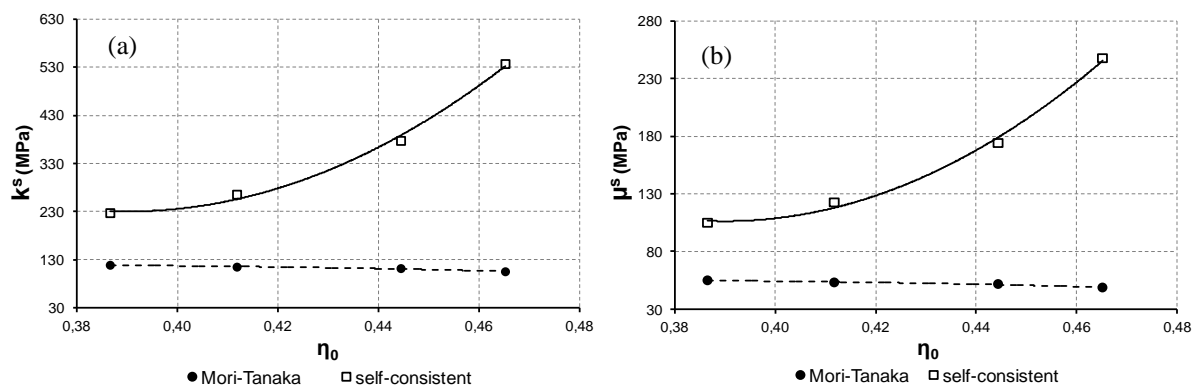


Figure 3: Bulk modulus  $k^s$  and shear modulus  $\mu^s$  of the fictitious solid phase derived from the Mori-Tanaka and self-consistent schemes.

The first observation is the remarkable difference between the results derived from the two schemes. The elastic moduli of fictitious solid phase predicted by the Mori-Tanaka scheme prove to be almost stable, independent on  $\eta_0$  within the investigated range of porosities. Actually, the moduli  $k^s$  and  $\mu^s$  are slightly decreasing functions of the porosity  $\eta_0$ . In this respect, they can be viewed as intrinsic values. In contrast, the self-consistent scheme leads to values of the fictitious solid elastic moduli that are significantly increasing with  $\eta_0$ . This variability observed in the case of self-consistent scheme proves disappointing. Nevertheless, the fictitious character of the solid phase that is at the basis of the model can explain the variability of  $k^s$  and  $\mu^s$  when the density of the original granular material is changing. It appears that the elastic behavior of the fictitious solid phase depends on the properties of both sand particles and intergranular interfaces. It also incorporates the effect of porosity, thus depending on the density of the granular assemblage.

## 4 ELASTIC PROPERTIES OF ACS

### 4.1 Micromechanical estimates of the bulk and shear moduli

After cement addition and curing period, the initial porous space of the sand is now partially filled with the hardened cement paste. The microstructure of the artificially cemented sand is then modeled a three-phase composite (Figure 4):

- The fictitious solid phase with volume fraction equal to  $1 - \eta_0$  and characterized by the elastic properties  $k^s$  and  $\mu^s$  evaluated in the previous section.
- The hydrated cement that is considered in the subsequent analysis as a rigid inclusion, i.e.  $k^c \sim \infty$  and  $\mu^c \sim \infty$ . Indeed, the Young modulus of a cement paste may reach values of a few tens GPa (Constantinides and Ulm, 2004; Wang et al., 1988), which is significantly higher than the elastic stiffness obtained for the fictitious medium. It is recalled that the order of magnitude of the latter is about a few hundreds MPa. The volume fraction of the hydrated cement is  $\eta_f - \eta_0$ , where  $\eta_f$  is the final porosity of the mixture.

- The residual porous phase. This phase corresponds to the pores originally present in the unreinforced material and that were not filled with hydrated cement particles after cement addition. The volume fraction of the porous phase (final porosity) is denoted by  $\eta_f$ . It is noted that  $\eta_f \leq \eta_0$ .

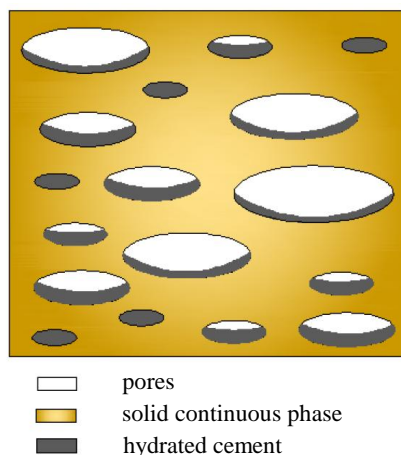


Figure 4: Schematic description of the artificially cemented sand.

In order to determine the elastic properties of the cemented sand, we again apply the linear homogenization method in which the phases are represented by spherical inclusions.

Adopting  $\zeta^0 = \zeta^s$  in Eq. 5 yields the Mori-Tanaka estimates of the bulk and shear moduli of ACS:

$$k_{MT}^{ACS} = \frac{1}{\mathcal{K}\left(\frac{\mu^s}{k^s}, \eta_0, \eta_f\right)} \mu^s \quad \text{with} \quad \mathcal{K}\left(\frac{\mu^s}{k^s}, \eta_0, \eta_f\right) = \frac{3}{4} \frac{3\eta_f + 4(1 - \eta_0 + \eta_f) \frac{\mu^s}{k^s}}{3(1 - \eta_f) + 4(\eta_0 - \eta_f) \frac{\mu^s}{k^s}} \quad (13)$$

$$\mu_{MT}^{ACS} = \frac{1}{\mathcal{M}\left(\frac{\mu^s}{k^s}, \eta_0, \eta_f\right)} \mu^s$$

$$\text{with} \quad \mathcal{M}\left(\frac{\mu^s}{k^s}, \eta_0, \eta_f\right) = \frac{4(2 - 2\eta_0 + 5\eta_f) \frac{\mu^s}{k^s} + 3(3 - 3\eta_0 + 5\eta_f)}{4(3 + 2\eta_0 - 5\eta_f) \frac{\mu^s}{k^s} + 3(2 + 3\eta_0 - 5\eta_f)} \times \frac{6 + 12 \frac{\mu^s}{k^s}}{9 + 8 \frac{\mu^s}{k^s}} \quad (14)$$

In the above equations, the elastic properties  $k^s$  and  $\mu^s$  of the fictitious solid phase should be substituted by their expressions determined in the previous section and given by Eq. 7 and Eq. 8.

Similarly the self-consistent estimates of the elastic properties of the ACS are derived by adopting  $\zeta^0 = \zeta^{\text{hom}}$  in Eq. 5.

$$k_{SC}^{ACS} = \frac{(1 - \eta_0)k^s}{1 + \alpha^{\text{hom}} \frac{k^s - k_{SC}^{ACS}}{k_{SC}^{ACS}}} + \frac{(\eta_0 - \eta_f)k_{SC}^{ACS}}{\alpha^{\text{hom}}} \quad \mu_{SC}^{ACS} = \frac{(1 - \eta_0)\mu^s}{1 + \beta^{\text{hom}} \frac{\mu^s - \mu_{SC}^{ACS}}{\mu_{SC}^{ACS}}} + \frac{(\eta_0 - \eta_f)\mu_{SC}^{ACS}}{\beta^{\text{hom}}} \quad (15)$$

with

$$\alpha^{\text{hom}} = \frac{3k_{SC}^{\text{ACS}}}{3k_{SC}^{\text{ACS}} + 4\mu_{SC}^{\text{ACS}}} \quad \text{and} \quad \beta^{\text{hom}} = \frac{6(k_{SC}^{\text{ACS}} + 2\mu_{SC}^{\text{ACS}})}{5(3k_{SC}^{\text{ACS}} + 4\mu_{SC}^{\text{ACS}})} \quad (16)$$

The elastic properties  $k^s$  and  $\mu^s$  of the fictitious solid phase that are involved in Eq. 15 and Eq. 16 should be substituted by their expressions given by Eq. 11. The homogenized bulk and shear moduli  $k_{SC}^{\text{ACS}}$  and  $\mu_{SC}^{\text{ACS}}$  are implicitly defined and their computation requires the resolution of a third-order polynomial equation.

## 4.2 Comparison with experimental results

This section is intended to assess the accuracy of the micromechanical predictions of ACS stiffness by comparison with the experimental measurements.

During the curing period, the hydration reaction between clinker and water (essentially setting and hardening phases) takes place and the anhydrous cement mixed with sand transforms in hydrated cement. An important issue is the preliminary evaluation of the volume of hydrated cement from the knowledge of anhydrous cement content in the mixture.

The simplest way to address the above issue is the Powers hydration model (Powers and Brownyard, 1947), which proves to be still relevant and remains widely used because of the easiness of its implementation. It provides the volume fraction of hydration products, including the volume fraction of hydrates that is of interest herein. The required information is the volume of hydrates  $\mathfrak{G}_h$  created when a unit volume of anhydrous cement is hydrated. Denoting by  $\varphi^h$  the volume fraction of hydrates formed at a given degree of hydration  $\xi$ , we have

$$\varphi^h = \mathfrak{G}_h \xi \varphi_0^a \quad (17)$$

where  $\varphi_0^a$  is the volume fraction of anhydrous cement initially mixed with sand, that is before the hydration reaction starts ( $\xi = 0$ ). This quantity is computed from the knowledge of the cement mass content.

In the case of artificially cemented soils, there is enough water than needed for complete hydration, and the reaction stops when all available anhydrous is consumed, i.e. when  $\xi = 1$ . This means that the volume fraction of hydrated cement after the process of curing is

$$\varphi^h = \mathfrak{G}_h \varphi_0^a \quad (18)$$

In the context of Powers model, we adopt  $\mathfrak{G}_h = 2.13$ .

The hydration being complete  $\xi = 1$ , all anhydrous cement present in the mixture transforms in hydrated cement. The final porosity is thus computed as

$$\eta_f = \eta_0 - \mathfrak{G}_h \varphi_0^a \quad (19)$$

The experimental results show that addition of cement increase significantly the stiffness of artificially cemented sand as compared to unreinforced sand. The gain in stiffness, defined by ratio  $\mu^{\text{ACS}} / \mu^{\text{sand}}$ , can reach values as high as 40 even for a moderate amount of cement characterized by a few percent cement mass content ( $\sim 7\%$ ). In contrast, the increase in the stiffness of ACS predicted by the micromechanical estimates remains significantly lower than that observed experimentally, thus indicating that the micromechanical model significantly underestimate the gain in stiffness induced by cement addition. This limitation can be

explained as follows.

The reinforcing effect induced by cement addition results from two mechanisms: a) the presence of hydrated cement particles that act as rigid inhomogeneities, and b) the process of cementation within sand that creates bonds and bridges between sand particles, imparting a kind of cohesion to the granular assemblage. In their original form, the two homogenization schemes used to estimate stiffness of ACS do not account for the second reinforcing mechanisms. A possible way to improve the micromechanical approach would consist in representing the hydrated cement phase within the REV as 3D interface (thin layers) surrounding the sand particles, similarly to the modeling proposed in [Maalej et al. \(2007\)](#) for assessing the strength properties of a sand reinforced by cement grouting.

Starting from the observation that the micromechanical modeling is not able to capture the effect of bonding induced by cementation, we adopt a heuristic reasoning which consists in affecting the analytical [Eq. \(13-16\)](#) by corrective terms

$$\bar{k}_{MT}^{-ACS} = f(\eta_f/\eta_0) \times k_{MT}^{ACS} \quad \bar{\mu}_{MT}^{-ACS} = f(\eta_f/\eta_0) \times \mu_{SC}^{ACS} \quad (20)$$

for the Mori-Tanaka estimates, and

$$\bar{k}_{SC}^{-ACS} = g(\eta_f/\eta_0) \times k_{MT}^{ACS} \quad \bar{\mu}_{SC}^{-ACS} = g(\eta_f/\eta_0) \times \mu_{SC}^{ACS} \quad (21)$$

for the self-consistent scheme.

The corrective functions  $f$  and  $g$  are fitted empirically to experimental data.

In the case of tested ACS specimen, a simple linear dependence on  $\eta_f/\eta_0$  has been chosen for both corrective functions

$$f(\eta_f/\eta_0) = a_{MT} (1 - \eta_f/\eta_0) + 1 \quad \text{and} \quad g(\eta_f/\eta_0) = a_{SC} (1 - \eta_f/\eta_0) + 1 \quad (22)$$

Scalars  $a_{MT}$  and  $a_{SC}$  are evaluated from data fitting. [Figure 5a](#) (resp. [Figure 5b](#)) shows, for the four tested sand materials, the evolution of  $\bar{\mu}_{MT}^{-ACS}$  (resp.  $\bar{k}_{MT}^{-ACS}$ ) as function of ratio  $\eta_f/\eta_0$ . The experimental results are also presented together with the corrected Mori-Tanaka estimates with  $a_{MT} = 129$ .

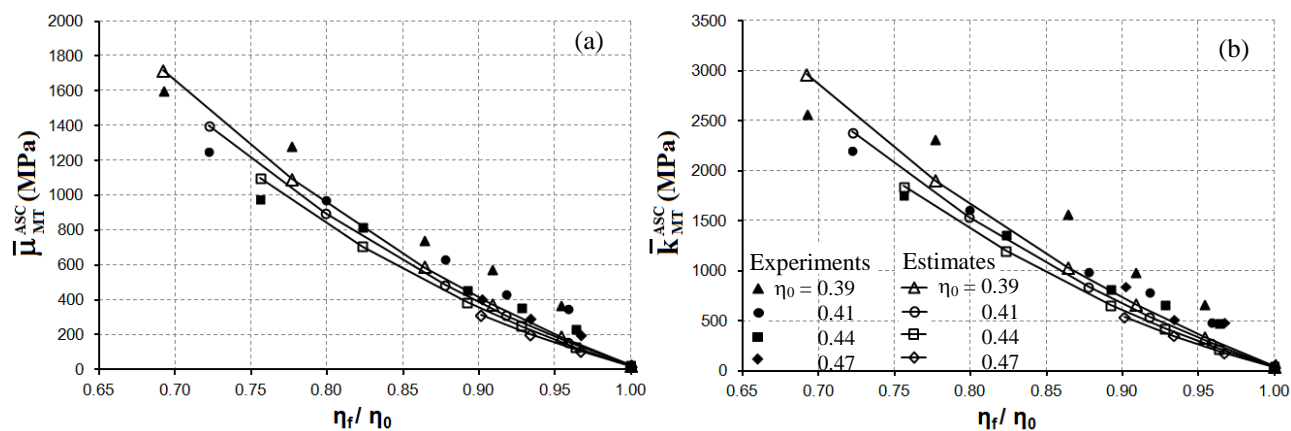


Figure 5: Mori-Tanaka estimates of ACS shear and bulk moduli and comparison with experimental results.

These figures clearly indicate that the introduction of corrective term [22](#) allows evaluating with a good accuracy the improvement in ACS stiffness that is induced by cement addition.

Similarly, the variations of homogenized shear modulus  $\bar{\mu}_{SC}^{-ACS}$  and bulk modulus  $\bar{k}_{SC}^{-ACS}$  derived from the self-consistent scheme versus  $\eta_f/\eta_0$  are shown Figure 6a and Figure 6b, together with the experimental results. The parameter  $a_{SC}$  defining the non-dimensional function  $g$  is taken as  $a_{SC} = 79$ .

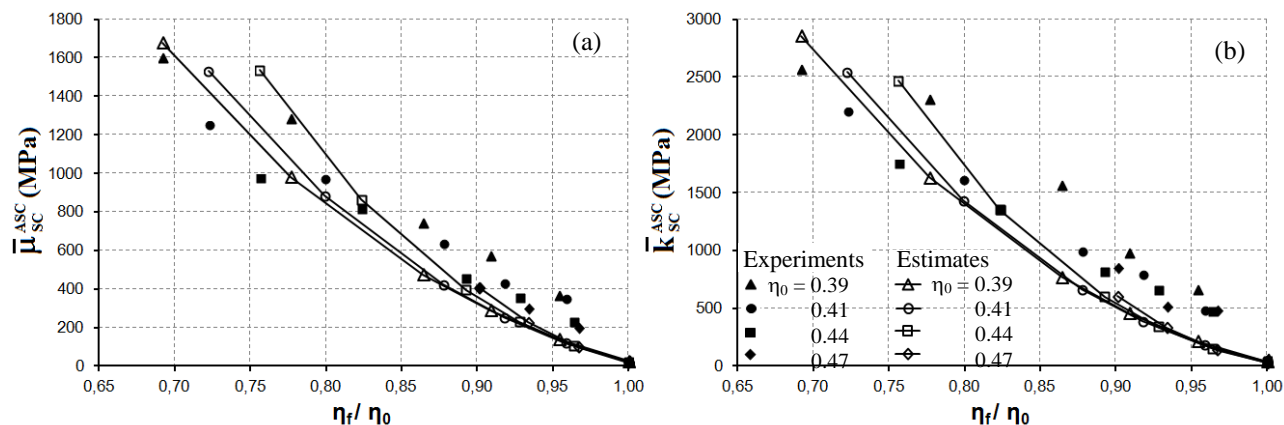


Figure 6: Self-consistent estimates of ACS shear and bulk moduli and comparison with experimental results.

A higher dispersion between micromechanical corrected predictions and experimental measurements is observed for the self-consistent estimates. This is probably the consequence of the low quality estimates of the fictitious medium stiffness ( $k^s$  and  $\mu^s$ ). As preliminary conclusion of the present elastic analysis, it seems that the Mori-Tanaka scheme is better adapted to capture the stiffness improvement brought by cement addition.

## 5 CONCLUSION

In this paper, a fundamental aspect of artificially cemented sand have been investigated by means of experimental tests and micromechanical-based modeling. Predictions of the effective elastic stiffness of ACS have been derived within the framework of continuum micromechanics and linear homogenization schemes. The estimates derived from the direct implementation of Mori-Tanaka and self-consistent schemes underestimate the increase in stiffening induced by cementation. Corrective terms have been therefore introduced and successively calibrated from the experimental data obtained by means of bender element tests performed on specimens of Osorio sand reinforced by different amounts of cement. It has been notably found from the comparison with experimental results that the empirically corrected Mori-Tanaka scheme is better indicated for capturing the stiffness improvement brought by cement addition.

Despite the theoretical model is not able to correctly capture the significant stiffening due to cementation, encouraging results have already been obtained. This feature should be improved through a more sophisticated description of the microstructure morphology. In particular, representing at the scale of REV cement past as 3D inter-phase surrounding the sand grains appears to be very promising for future extensions aiming at further enhancing micromechanics-based elasticity model for ACS.

Further efforts can be devoted to address to the following issues:

- Porosity of ACS has been evaluated based on the assumption that the in initial pore space of sand is partially filled by hydrated cement and the volume of the latter was computed

using the Powers model. Experimental data based for instance on mercury intrusion porosimetry tests would be valuable to support the relevance of the theoretical evaluation.

- A key challenge lies in the assessment of hydraulic conductivity of ACS by means of micromechanics-based approaches. Experimental analyzes (e.g. Saada et al. (2005)) have shown that very small amounts of cement may reduce significantly the permeability of ACS when compared to sand. This reduction is explained by the fact that hydraulic access to a pore can be prevented by cement particles, which cannot be accounted for easily by means of classical homogenization schemes.

- Effect of curing time on the elastic and strength properties, together with their evolution in time is also relevant to ACS mechanical modeling. Ongoing research in this direction is expected to provide in the next future preliminary answers to this question (Consoli et al., 2013).

It is believed that the homogenization approach supported by appropriate experimental data provides a promising framework for reliable modeling in the field of reinforced granular media.

## ACKNOWLEDGMENTS

The authors gratefully appreciated the financial support provided by the Brazilian Federal Agency CAPES (Coordenação de Aperfeiçoamento de Pessoal de Nível Superior) and Brazilian Research Council CNPq (Conselho Nacional de Desenvolvimento Científico e Tecnológico).

## REFERENCES

- American Society for Testing and Materials (ASTM). *Standard classification of soils for engineering purposes*, ASTM D 2487-93. West Conshohocken, PA: ASTM International, 1993.
- American Society for Testing and Materials (ASTM). *Standard specification for Portland cement*, ASTM C 150-09. West Conshohocken, PA: ASTM International, 2009.
- Benveniste, Y. A new approach to the application of Mori-Tanaka's theory in composite materials. *Mechanics of Materials*, 6: 147-157, 1987.
- Bouchelaghem, F., Benhamidab, A. and Quoc Vub, H. Nonlinear mechanical behaviour of cemented soils. *Computational Materials Science*, 48: 287-295, 2010.
- Budiansky, B. On the elastic moduli of some heterogeneous materials. *Journal of the Mechanics and Physics of Solids*, 13: 223-227, 1965.
- Clayton, C. R. I. Stiffness at small strain: research and practice. *Geotechnique*, 61: 5-37, 2011.
- Consoli, N. C., Rotta, G. V. and Prietto, P. D. M. Yielding-compressibility-strength relationship for an artificially cemented soil cured under stress. *Geotechnique*, 56: 69-72, 2006.
- Consoli, N. C., Foppa, D., Festugato, L. and Heineck, K. S. Key parameter for strength control of artificially cemented soils. *Journal of Geotechnical and Geoenvironmental Engineering*, 133: 759-763, 2007.
- Consoli, N. C., Cruz, R. C., Floss, M. F., Foppa, D. and Festugato, L. Parameters controlling tensile and compressive strength of artificially cemented soils. *Journal of Geotechnical and Geoenvironmental Engineering*, 136: 197-205, 2010.
- Consoli, N. C., Fonseca, A. V., Caberlon, R.C. and Fonini, A. Parameters Controlling

- Stiffness and Strength of Artificially Cemented soils. *Geotechnique*, 62: 177-183, 2012a.
- Consoli, N. C., Fonini, A., Maghous, S. and Schnaid, F. Experimental analysis of the mechanical properties of artificially cemented sands and their evolution in time. *Proceedings of the 18th International Conference on Soil Mechanics and Geotechnical Engineering* (accepted paper), Paris, 2013.
- Constantinides, G. and Ulm, F-J The effect of two types of C-S-H on the elasticity of cement-based materials: Results from nanoindentation and micromechanical modeling. *Cement and Concrete Research*, 34: 67–80, 2004.
- Dormieux, L., Kondo, D. and Ulm, F-J. *Microporomechanics*, John Wiley & Sons, 2006a.
- Dormieux, L., Sanahuja, J. and Maghous, S. Influence of Capillary Effects on Strength of Non-Saturated Porous Media. *Comptes Rendus Mécanique*, 334: 19-24, 2006b.
- Emeriault, F. and Cambon, B. Micromechanical modeling of anisotropic non-linear elasticity of granular medium. *International Journal of Solids Structures*, 33: 2591-2607, 1996.
- Eshelby, J. D. The determination of the elastic field of an ellipsoidal inclusion, and related problems. *Proceedings of the Royal Society of London A* 241, 1226: 376-396, 1957.
- Hill, R. A self-consistent mechanics of composite materials. *Journal of the Mechanics and Physics of Solids* 13: 213–222, 1965.
- Maalej, Y. Comportement mécanique d'un milieu granulaire injecté par un coulis de ciment: étude expérimentale et modélisation micromécanique. PhD thesis (in french). Paris: Ecole Nationale des Ponts et Chaussées, 2007.
- Maalej, Y., Dormieux, L., Canou, J. and Dupla, J. C. Strength of a granular medium reinforced by cement grouting. *Comptes Rendus Mécanique* 335: 87–92, 2007.
- Maghous, S., Saada, Z., Dormieux, L., Canou, J. and Dupla, J.-C. A model for in situ grouting with account for particle filtration. *Computers and Geotechnics*. 34: 164-174, 2007.
- Mitchell, J. K. Soil improvement – State-of-the art report. Proc. *10th Int. Conf. on Soil Mechanics and Foundation Engineering*, Balkema, Rotterdam, Netherlands, 509-565, 1981.
- Mori, T. and Tanaka, K. Average stress in matrix and average elastic energy of materials with misfitting inclusions. *Acta Metallurgica* 21: 571-574, 1973.
- Mura, T. *Micromechanics of Defects in Solids*, 2nd edn. Netherlands: Martinus Nijhoff Publishers, 1987.
- Powers, T. C. and Brownyard, T. L. Studies of the physical properties of hardened Portland cement paste (nine parts). *Journal of the American Concrete Institution*, 43: 101-132, 1946.
- Saada, Z., Canou, J., Dormieux, L., Dupla, J.-C. and Maghous, S. Modelling of cement suspension flow in granular porous media. *International Journal for Numerical and Analytical Methods in Geomechanics*, 29: 691-711, 2005.
- Suquet, P. M. Elements of homogenization for inelastic solid mechanics, Homogenization Techniques for Composite Media. *Lecture notes in physics* 272: E. Sanchez-Palencia, A. Zaoui (Eds), Springer, New York, 193-278, 1987.
- Viggiani, G. and Atkinson, J.H. Stiffness of fine-grained soils at very small strains. *Geotechnique*, 45: 249–265, 1995.
- Wang, J. A.; Lubliner, J. and Monteiro, P. J. M. Effect of ice formation on the elastic moduli of cement paste and mortar. *Cement and Concrete Research*, 18: 874–885, 1988.
- Zaoui, A. Continuum Micromechanics: Survey. *Journal of Engineering Mechanics*, 128: 808-816, 2002.